Title: Rapid Activation of Hematopoietic Stem Cells

Authors: Roshina Thapa[1,2] and Erez Elfassy[1,2,*], Leonid Olender[1], Omri Sharabi[1], Roi Gazit[1*]

Affiliations:
[1] The Shraga Segal Department of Microbiology, Immunology, and Genetics; Faculty of Health Sciences; National Institute for Biotechnology in the Negev; The Ben-Gurion University of the Negev, Israel POB 84105

[2] These authors contributed equally
* Correspondence: elfassye@post.bgu.ac.il (E.F.), gazitroi@bgu.ac.il (R.G.)

Keywords
Hematopoietic Stem Cells, HSC, Activation Markers, Rapid Activation, CD69, CD317, BST2, Ki67, Differentiation, Proliferation.

Summary:

Adult Hematopoietic Stem Cells (HSCs) are quiescent in the bone marrow (BM). Following perturbations, such as blood loss or infection, HSCs may activate to accelerate the production of needed effector blood and immune cells. Surprisingly little is known about the earliest stages of HSCs activation. We utilize surface markers of HSC activation, CD69 and CD317, revealing very early response in as little as 2 h. The dynamic expression of HSC activation markers varies between viral-like (poly-Inosinic-poly-Cytidylic) or bacterial-like (Lipopolysaccharide) immune stimuli. We further quantify the dose-response, demonstrating a low-threshold and similar sensitivity of HSCs like other progenitors in the BM. Finally, we find a positive correlation between surface activation markers expression and the early exit from quiescence into proliferation following immune stimulation. Our data show that premier response of adult stem cells to immune stimulation is rapid, sensitive, and directly leading towards proliferation.

Introduction

Hematopoietic Stem Cells (HSCs) are the source for all blood and immune cells (Sawai et al., 2016) (Yamamoto et al., 2018). HSCs are largely quiescent in the adult bone marrow (BM), preserving long-term multipotency (Busch et al., 2015; Dzierzak and Speck, 2008; van der Wath et al., 2009; Yamazaki et al., 2007). Upon need, HSCs may gain activation, proliferate, and contribute to the accelerated hematopoiesis (Khosravi et al., 2014; Takizawa et al., 2011). How fast, and how sensitive the activation of HSCs is yet to be determined.

Immune activation by poly-Inosinic-poly-Cytidylic (pIpC), or by Lipopolysaccharide (LPS), are most useful for viral- or bacterial-like immune stimuli (Chavakis et al., 2019). pIpC stimulation activates type-I interferons and activates HSCs in the BM (Essers et al., 2009; Sato et al., 2009). The activation is largely IFNα (Essers et al., 2011; Essers et al., 2009). Interestingly, pIpC was reported to not only activate, but to also skew differentiation into megakaryocytes (Haas et al., 2015), presumably to enhance coagulation. Moreover, chronic pIpC stimulation was shown to drive DNA-damage and possible exhaustion of genetically susceptible HSCs (Walter et al., 2015), while chronic viral infection impairs HSC's potency indirectly via CD8 T cells that change the BM niche (Isringhausen et al., 2021). LPS activates the major TLR4-pathway, and activates HSCs directly and indirectly (Takizawa et al., 2017; Takizawa et al., 2011). Overwhelming stimulation can exhaust HSCs (Baldridge et al., 2010; de Bruin et al., 2013; Matatall et al., 2016; Pietras et al., 2016); however, milder models suggest that HSCs may re-enter quiescence and preserve potency despite prolonged stimulation (Pietras et al., 2014). Interestingly, LPS and related cytokines such as IL-1 and TNFα can skew differentiation into the myeloid rather than the lymphoid branch (Pietras et al., 2016; Takizawa et al., 2017; Yamashita and Passegue, 2019). Immune stimulation was further reported to induce trained immunity in HSCs including metabolic and epigenetic myeloid skew (de Laval et al., 2020; Mitroulis et al., 2018). Either viral- or bacterial stimuli induce the quiescent HSCs to proliferate – and give rise to more effector cells (Essers et al., 2011; Pietras et al., 2014; Takizawa et al., 2017; Takizawa et al., 2011; Walter et al., 2015; Yanez et al., 2009). Surprisingly, while previous studies extensively studied the days and months following immune stimulation, the acute early stages of HSC's activation are relatively less studied.

We identified HSC-activation markers (Bujanover et al., 2018), including CD69 (*Clec2c*) and CD317 (*Bst2*). These were validated in a brilliant study showing the essential role of CD317 (also called BST2) for retaining activated HSCs in the proper BM niche (Florez et al., 2020). We sought to utilize these surface markers to study how early HSC activation occur and how sensitive HSCs

are to commonly used immune stimuli. The quantified data show rapid and sensitive responses, with a positive correlation between surface markers and the proliferative state of HSCs in the BM.

Results

Immune activation of hematopoietic stem and progenitor cells is rapid

We previously showed that HSC activation markers CD69 and CD317 are expressed at 24 h following immune stimulation (Bujanover et al., 2018). However, we did not find data on HSC response at earlier time points. We sought to utilize these markers for the study of earlier time points. Refining the time scale analysis of HSCs activation may reveal how fast they respond to the immune stimuli. Therefore, we stimulated mice with pIpC (100 µg, Intra-Peritoneal) and collected BM for FACS analysis using conventional HSC markers (see methods) plus CD69 and CD317 at 2, 4, and 24 h (Figure 1A). We observed an elevation of CD69 expression to more than 30% of the Lineage$^-$ Sca1$^+$ cKit$^+$ (LSK) compartment and in the HSC LSK_CD48$^-$150$^+$ population after 2 h (Figure 1B). CD69 expression further increased at 4 and 24 h (Figures 1C and1D). Intriguingly, CD317 expression seems to increase a bit slower, as seen at 2 and 4 h, with a peak at 24 h (Figures 1C and 1D). Regarding CD317 expression, the BM progenitor populations showed a similar trend. Yet, it is important to notice that although CD317 expression on Lin$^-$ population is with a comparable time-dependent scale, the magnitude of activation is noticeably different. The more primitive populations, such as LSK and HSC LSKCD48$^-$150$^+$, are far more sensitive to immune stimulation. In the case of pIpC stimulation, after 24 h, more than 80% of HSC LSKCD48$^-$150$^+$ and almost 100% of LSK cells elevate their CD317 expression. On the other hand, less the 60% of Lin$^-$ and less than 80% of Lineage$^-$cKit$^+$ (LK) cells express CD317 after 24 h (Figures S1A-S1C). It is worth noticing that pIpC stimulation causes an elevation of Sca-1 expression at the later time point, shifting more progenitors into the LSK gate at the 24 h.

The pIpC mimics viral infection, we also wanted to examine a model for bacterial infection. LPS activates TLR4 and can activate HSCs both directly and indirectly. We used a dose of 20 µg, injected IP (Figure 1E). With this stimulation, CD69 expression peaked at 2 h, both in the LSK and in the HSC LSKCD48$^-$150$^+$ populations, gaining about 90% positive cells (Figure 1G). However, with LPS stimulation, CD317 reached similar expression levels only at 4 h. Later, CD69 expression decreased, whereas CD317 levels were maintained in most of the cells (Figures 1F-H). Furthermore, the elevation of CD69 and CD317 expression in other populations in the BM of the same mice were substantial as well (Figures S1D-F). Lin$^-$ population, again, follows the same time-dependent trend in expression of both CD69 and CD317, peaking after 2 and 4 h respectively, but

to a level of about 40% of cells (Figures S1D and S1E), followed by a decrease in expression in agreement with previous data (Bujanover et al., 2018). In the case of the LK population, the baseline of CD69 expression is in 25% of cells and peaks at 4 h to more than 60% of the cells. CD317 expression elevates after 4 h to about 90% of the cells. Both CD69 and CD317 expression decrease after 24 h, with CD69 levels returning to baseline levels and CD317 remains in about 60% of the cells (Figures S1D and S1F). It is important to notice that LPS stimulation, like pIpC stimulation, causes an elevation of Sca-1 expression, meaning that part of the observed LSK cells is due to the pIpC stimulation. These findings suggest CD69 to be more responsive during the early phase of immune stimulation (2 h), whereas CD317 is more responsive towards the later phase of immune stimulation (24 h). These findings also indicate that primitive populations are more sensitive to immune stimulation.

CD317 reveals a dose-response to pIpC above a minimal threshold

Following the findings of rapid response to pIpC and accumulation of CD317 at 24 h, we next wanted to examine if HSCs activation is dose-dependent or rather an all-or-none response. To test this hypothesis, we challenged mice with various doses of pIpC, ranging from 0.01 µg to 100 µg, and analyzed the expression of CD317 in different populations of BM cells. The CD317 expression in the broader LSK and the HSC LSKCD48-150+ was proportional to an increasing dose of pIpC such that 0.1 µg of pIpC is the minimal dose for CD317 expression, and subsequent increase in pIpC dose enhanced CD317 expression to 80% (Figures 2A-C). The minimal dose of pIpC observed in our study was further endorsed from the EC50 calculation to be 0.10 µg for LSK and 0.12 µg for HSC LSKCD48^{-}150^{+}. Furthermore, the relationship between pIpC dose and CD317 expression fit well with linear regression (Figures 2D and 2E). Similarly, Lin- or LK cells followed a similar incremental trend in CD317 expression with pIpC (Figure S2). However, the magnitude of increment observed within the Lin- population was much lower (expression increased to 40% with the highest dose of pIpC) than the magnitude of increment observed in broader LSK and the HSC LSKCD48-150+ (expression increased to 80% with the highest dose of pIpC, Figures 2 and S2). Remarkably, the LK cell population showed stronger response relative to the Lin- population, with CD317 overexpression reaching around 60% with the highest dose of pIpC (Figure S2). Furthermore, calculating EC50 value of CD317 activation for Lin- and LK populations again fit well with linear regression, and found to be 0.07 µg and 1.30 µg, respectively (Figure S2D and S2E). Therefore, Stem- and progenitors have dose-response to pIpC throughout a broad range of concentrations.

CD69 elevation is dose-dependent at higher concentrations of LPS stimulation

Next, following the robust response seen before (Figure 1), we examined the dose-dependent effect of LPS on CD69 expression. We challenged mice with various doses of LPS (0.0001-20 µg) for 2 h and analyzed the expression of CD69 in different populations of BM cells. The CD69 expression in the LSK and the HSC LSKCD48$^-$150$^+$ populations was significantly upregulated at relatively higher doses of LPS (0.1 µg onwards), with maximal upregulation observed at 1 µg of LPS. More specifically, in the LSK population, 50% of cells showed CD69 expression with 0.1 µg of LPS, which increased up to 80% with 1 µg of LPS (Figures 3A and 3B). Similarly, CD69 expression in the HSC LSKCD48$^-$150$^+$ population increased from 25% to 60% with 0.1 to 1 µg of LPS (Figures 3A and 3C). The EC_{50} value of 0.07 µg (LSK), and 0.21 µg (HSC LSKCD48$^-$150$^+$), delineated a threshold for LPS on CD69 elevation in these populations. Nevertheless, we gained clear dose-response with the higher LPS concentration and CD69 activation using the linear regression tool (Figure 3D and3E). Furthermore, the relatively high-threshold for LPS was even more pronounced in the Lin$^-$ or LK populations, such that only 1µg of LPS was able to exert a significant effect on the expression of CD69, with the overall increment reaching up to 20% with 20 µg of LPS, as seen in (Figures S3A-S3C). Importantly, despite having a lower maximal-activation in the Lin$^-$ or LK, the EC_{50} values of 0.39 µg (Lin$^-$), and 0.17 µg (LK) are in the same range as LSK or HSCs (Figures S3D and S3E).

CD69 and CD317 expression in activated stem and progenitor populations positively correlate with proliferation

To evaluate whether elevation in activation markers correlates with hematopoietic stem and progenitor cell proliferation, we conducted a cell cycle analysis. In this set of experiments, we tested for Ki67 expression in pIpC and LPS stimulated mice at 2 and 24 h or 4 and 24 h, respectively (Figures 4A and 4D). After immune stimulation, we extracted the BM, stained with extracellular markers, fixed and permeabilized the cells, and stained with the nuclear Ki67 marker for proliferation (see methods). Surprisingly, at 4 h post pIpC stimulation, a significant proportion of LSKCD317$^+$ cells were observed in the S and M phase of the cell cycle, more than LSKCD317$^-$ cells. The CD317$^+$ fraction had less cells in the G0 phase, and this trend was sustained at 24 h (Figure 4B and 4C). Likewise, similar division kinetics were observed between Lin$^-$CD317$^+$ populations and activated LSK and HSC LSKCD48$^-$150$^+$ 317$^+$ (activated) populations; a significant number of activated LK cells were found to be more proliferative at both 4 and 24 h, as evident with a reduction in G0 phase and elevation of S/M when compared to the CD317$^-$ fraction of the LK cell population (Figures S4A-S4C).

We also tested the correlation between CD69 expression and proliferation following LPS stimulation. Here only a small change was observed in the LSK population at 2 h, reaching better significance at 24 h, with $CD69^+$ being less quiescent and more proliferating (Figure 4E). Surprisingly, within HSC $LSKCD48^-150^+69^+$ we observed more G0 than counterpart $CD69^-$ at the early 2 h time point (Figure 4F). At 24 h the $CD69^+$ HSCs were not more proliferating than the $CD69^-$, although they equal the G0 fraction (Figure 4F). At the early 2 h time point, the broader Lin^- and LK populations showed significantly more proliferation of the $CD69^+$ fraction (Figure S4E). But at 24 h the Lin^- showed no significant difference, and the LK $CD69^+$ elevated proliferation was only slightly more than the $CD69^-$ fraction (Figure S4F). Taken together, with one peculiar exception of HSCs at early 2 h time point, our data demonstrate the positive correlation of surface activation markers and proliferation of stem or progenitors following pIpC and LPS stimulation.

Discussion

In this study, we present the rapid activation of HSCs following immune activation *in vivo*. Utilizing surface markers, we demonstrate that HSCs gain rapid activation after 2 h. We show high sensitivity to both pIpC and LPS, with a dose-response range and a possible low threshold. Finally, we find that surface activation markers correlated with the proliferative state, suggesting that the exit from quiescence is faster than previously estimated.

The immune response is rapid, showing pronounced elevation of systemic inflammatory cytokines by 2 h (Copeland et al., 2005). HSCs may sense immune activation both directly and indirectly, involving multiple receptors for microbial products (TLRs) and cytokines receptors for IL-1, IL-6, TNFα, and IFN (Chavakis et al., 2019; Clapes et al., 2016). As the key role of HSCs is to produce more cells, previous studies focused on their proliferation and differentiation following immune stimulation (Chavakis et al., 2019). Surface activation markers allow us to quantify earlier stages with single-cell resolution (Figure 1). CD317 (BST2) has a role in anti-viral response (Le Tortorec et al., 2011), and it was also shown to retain HSCs in the BM(Florez et al., 2020). CD69 is a major activation marker of immune cells and a metabolic regulator (Cibrian and Sanchez-Madrid, 2017); intriguingly, CD69 is also implicated in HSPC retention in the BM (Notario et al., 2018), suggesting that CD69 like CD317 may regulate BM localization following stimulation.

Realizing the fast activation by 2 h position HSCs at the front-line of the immune response, even at their BM-niche. A front-line role was suggested for HSPCs in peripheral, secondary lymphoid tissues (Massberg et al., 2007). In this study, we focus on the BM, where most adult HSCs reside.

Intriguingly, the sensitivity of HSCs is comparable to other progenitors in the BM (Figures 2 and 3) and other effector immune cells *in vivo* (Poast et al., 2002; Raveche and Steinberg, 1982; Tough et al., 1997); suggesting for a coordinated systemic response. Thus, our data point for HSCs to be an integral part of the immune response; not a distal reservoir called at later stages, but a proximal part of the acute response to stimulation.

The activation of HSCs might have later consequences. Trained immunity, which is the adapted immunity of myeloid cells, suggests fine-tuning of response (de Laval et al., 2020). It will be most interesting to realize how deep trained immunity is within the hematopoietic hierarchy. Our data suggest that HSCs do sense and gain rapid activation at a low threshold, providing possible "training" through multiple experiences throughout life. Intriguingly, the aging of HSCs is intrinsic (Rossi et al., 2005), but not yet realized at the molecular level. HSCs were suggested to count cell divisions (Bernitz et al., 2016; Haas et al., 2018) – thus, proliferation must be carefully regulated. Indeed, we recently reported that HSCs may ignore an acute hypersensitivity immune response (Bujanover et al., 2021). Importantly, blocking inflammation was shown to attenuate the deleterious impact on HSPCs (Hernandez et al., 2019), providing strong support to prophylactic treatments. This study quantifies the rapid response of HSCs and provides further options to study modulation to either enhance or restrain the activation of our long-term multipotent reservoir for blood and immune cells.

Limitations

The prospective isolation of HSCs allowed major advancements, but some of the markers do change following immune stimulation, as we and others reported (Bujanover et al., 2018). A recent study suggests an improved protocol adding both CD34 and EPCR markers to better identify functional HSCs following immune stimulation (Rabe et al., 2020). We choose to use the common gating of LSKCD48$^-$CD150$^+$ as we focus on early time points. Also, we limited to BM and did not explore HSC mobilization, which may occur at later time points. Notably, the best isolated HSCs might consist of 1/3 functional long-term reconstituting cells, and as a population, these HSCs are heterogeneous (Haas et al., 2018). Our data show that virtually all the LSKCD48$^-$CD150$^+$ population, which encompass all HSCs, gain activation markers. We also limit our experiments to key time points, reducing the number of animals. Future studies may fine-tune the time course and further examine possible heterogeneity among earlier- and later-activated HSCs and progenitors.

STAR★Methods

Key resource table

REAGENT or RESOURCE	SOURCE	IDENTIFIER
Antibodies		
Lineage Cocktail-PacBlue	BioLegend	Cat# 133310, N/A
Lineage-A700	BioLegend	Cat# 652419, RRID:AB_2564284
Sca1-APC	BioLegend	Cat# 108112, RRID:AB_313349
cKit-APCcy7	BioLegend	Cat# 105826, RRID:AB_1626278
CD150-PeCy7	BioLegend	Cat# 115914, RRID:AB_439797
CD48-PerCP/cyanine5.5	BioLegend	Cat# 103422, RRID:AB_2075051
CD69-FITC	BioLegend	Cat# 104506, RRID:AB_313109
CD317-PE	BioLegend	Cat# 127010, RRID:AB_1953285
DAPI	BioLegend	Cat# 422801. N/A
Ki67-FITC	BioLegend	Cat# 652410, RRID:AB_2562141
Ki67-PE	BioLegend	Cat# 652404, RRID:AB_2561525
Chemicals, peptides, and recombinant proteins		
Polyinosinic–polycytidylic acid sodium	Invivogen, High Molecular Weight	tlrl-pic-5
Lipopolysaccharides of *E. coli* O55:B5	Sigma-Aldrich	L2880
Ficoll-Paque™ premium 1.084	Cytiva	17544602
TWEEN 20	Sigma-Aldrich	P1379
Paraformaldehyde	EM Sciences	15710
Experimental models: Organisms/strains		
Mouse: C57BL/6J	Jax lab	Local breed
Software and algorithms		
Graph Pad Prism5	GraphPad Software	www.graphpad.com
Adobe IllustratorC5	Adobe Illustrator software	www.adobe.com
BioRender	BioRender	BioRender.com

Mice and Ethical

All mice were kept at the Ben-Gurion University SPF (specific pathogen-free) unit. Mice strains used were C57Bl/6. Both male and female mice at 8-12 weeks old were used for the experiments, with age- and gender-matched littermates as control. All experiments were carried out according to the guidelines of the ethical committee and after approval of the local and state IACUC (IL-68-11-2018-D).

Immune stimulation

Mice were stimulated by poly-Inosinic–poly-Cytidylic acid sodium (pIpC: Invivogen, High Molecular Weight, catalog code: trl-pic-5) intraperitoneally (i.p.) 100 µg per mouse. Lipopolysaccharides of *E. coli* O55:B5 (LPS, Sigma-Aldrich cat: L2880 lot: 113M4068V) were

administered i.p. at 20 µg per mouse. Stimulation was done at various time points (2, 4, and 24 h). Unstimulated mice were used as control, such as time 0. For dose-response, mice were stimulated by Polyinosinic–polycytidylic acid sodium salt (pIpC: Invivogen, High Molecular Weight, catalog code: tlrl-pic-5) intraperitoneally (i.p.) with various doses (0.01, 0.1, 1, and 10 µg), and analyzed at 24 h. Unstimulated mice were used as control. Lipopolysaccharides of *E. coli* O55:B5 (LPS, Sigma-Aldrich cat: L2880 lot: 113M4068V) were administered i.p. with various doses (0.0001, 0.001, 0.01, 0.1, and 1 µg) per mouse, and analyzed at 2 h.

Flow cytometry

BM cells were extracted from the tibia, femur, and pelvis using mortar and pestle; sample media comprised of Phosphate Buffer Saline (PBS) with 2mM EDTA and 2% Foetal Bovine Serum (FBS Lot#2137767, Biological Industries). Mononuclear cells were enriched over Ficoll-Paque™ premium 1.084 (Cytiva, cat #17544602) and stained using the following antibodies (all from Biolegend): Lineage Cocktail-PacBlue, Lineage-A700, Sca1-APC, cKit-APCcy7, CD150-PeCy7, CD48-PerCP/cyanine5.5, CD69-FITC, CD317-PE, and DAPI. FACS Cytoflex LX (Beckman Coulter) and FacsAriaIII (BD) were used for analysis and sorting. Cytexpert software was used to analyze and visualize FACS data.

Cell cycle analysis

BM cells were extracted from the tibia, femur, and pelvis; mononuclear cells were enriched over histopaque and stained: Lineage-A700, Sca1-APC, cKit-APCCy7, CD150-PECy7, CD48-PC5.5, CD69-FITC, and CD317-PE. Cells were fixated in a 96U plate in 250 µl of 2% paraformaldehyde (PFA, EMS #15710) in PBS at room temperature for 20 min, washed twice in PBS, permeabilized in 0.25%Tween 20 (Sigma-Aldrich, P1379) in PBS for 30min, washed twice in 0.1% tween PBS then stained by Ki67-FITC or Ki67-PE (Biolegend) in 1:300 of stock in 0.1% tween PBS over-night. DAPI (10 µg/ml) was added to the cells before flow-cytometric analysis.

Statistics

FACS data are shown as mean ± SD. Data are representative of at least three independent experiments unless otherwise noted. A two-tailed T-test was performed, with $p < 0.05$ considered significant. Linear regression statistical tool was performed using the Graphpad prism.

Acknowledgments

We thank all members of the R.G. laboratory for helpful discussions. Grant support MOST-DKFZ#CA179, and ISF#883/21.

Contributions

EE and RT performed experiments and collected data; EE, RT, LO and OS analyzed and interpreted data; RG concept and designed the study; EE, RT, and RG wrote the manuscript.

Declaration of interests

All authors declare no competing interests.

References

Baldridge, M.T., King, K.Y., Boles, N.C., Weksberg, D.C., and Goodell, M.A. (2010). Quiescent haematopoietic stem cells are activated by IFN-gamma in response to chronic infection. Nature *465*, 793-797.

Bernitz, J.M., Kim, H.S., MacArthur, B., Sieburg, H., and Moore, K. (2016). Hematopoietic Stem Cells Count and Remember Self-Renewal Divisions. Cell *167*, 1296-1309 e1210.

Bujanover, N., Goldstein, O., Greenshpan, Y., Turgeman, H., Klainberger, A., Scharff, Y., and Gazit, R. (2018). Identification of immune-activated hematopoietic stem cells. Leukemia *32*, 2016-2020.

Bujanover, N., Thapa, R., Goldstein, O., Olender, L., Sharabi, O., Milsom, M.D., and Gazit, R. (2021). Hypersensitivity response has negligible impact on Hematopoietic Stem Cells. Stem Cell Reports *16*, 1884-1893.

Busch, K., Klapproth, K., Barile, M., Flossdorf, M., Holland-Letz, T., Schlenner, S.M., Reth, M., Hofer, T., and Rodewald, H.R. (2015). Fundamental properties of unperturbed haematopoiesis from stem cells in vivo. Nature *518*, 542-546.

Chavakis, T., Mitroulis, I., and Hajishengallis, G. (2019). Hematopoietic progenitor cells as integrative hubs for adaptation to and fine-tuning of inflammation. Nat Immunol *20*, 802-811.

Cibrian, D., and Sanchez-Madrid, F. (2017). CD69: from activation marker to metabolic gatekeeper. Eur J Immunol *47*, 946-953.

Clapes, T., Lefkopoulos, S., and Trompouki, E. (2016). Stress and Non-Stress Roles of Inflammatory Signals during HSC Emergence and Maintenance. Frontiers in immunology *7*, 487.

Copeland, S., Warren, H.S., Lowry, S.F., Calvano, S.E., Remick, D., Inflammation, and the Host Response to Injury, I. (2005). Acute inflammatory response to endotoxin in mice and humans. Clin Diagn Lab Immunol *12*, 60-67.

de Bruin, A.M., Demirel, O., Hooibrink, B., Brandts, C.H., and Nolte, M.A. (2013). Interferon-gamma impairs proliferation of hematopoietic stem cells in mice. Blood *121*, 3578-3585.

de Laval, B., Maurizio, J., Kandalla, P.K., Brisou, G., Simonnet, L., Huber, C., Gimenez, G., Matcovitch-Natan, O., Reinhardt, S., David, E.*, et al.* (2020). C/EBPbeta-Dependent Epigenetic Memory Induces Trained Immunity in Hematopoietic Stem Cells. Cell Stem Cell *26*, 657-674 e658.

Dzierzak, E., and Speck, N.A. (2008). Of lineage and legacy: the development of mammalian hematopoietic stem cells. Nat Immunol *9*, 129-136.

Essers, M., Lutz, R., Thamm, S., Uckelmann, H., Wurzer, S., and Trumpp, A. (2011). Stress-Induced Activation of Dormant Hematopoietic Stem Cells In Vivo. Blood *118*, 1453-1453.

Essers, M.A., Offner, S., Blanco-Bose, W.E., Waibler, Z., Kalinke, U., Duchosal, M.A., and Trumpp, A. (2009). IFNalpha activates dormant haematopoietic stem cells in vivo. Nature *458*, 904-908.

Florez, M.A., Matatall, K.A., Jeong, Y., Ortinau, L., Shafer, P.W., Lynch, A.M., Jaksik, R., Kimmel, M., Park, D., and King, K.Y. (2020). Interferon Gamma Mediates Hematopoietic Stem Cell Activation and Niche Relocalization through BST2. Cell reports *33*, 108530.

Haas, S., Hansson, J., Klimmeck, D., Loeffler, D., Velten, L., Uckelmann, H., Wurzer, S., Prendergast, A.M., Schnell, A., Hexel, K.*, et al.* (2015). Inflammation-Induced Emergency Megakaryopoiesis Driven by Hematopoietic Stem Cell-like Megakaryocyte Progenitors. Cell Stem Cell *17*, 422-434.

Haas, S., Trumpp, A., and Milsom, M.D. (2018). Causes and Consequences of Hematopoietic Stem Cell Heterogeneity. Cell Stem Cell *22*, 627-638.

Hernandez, G., Mills, T.S., Rabe, J.L., Chavez, J.S., Kuldanek, S., Kirkpatrick, G., Noetzli, L., Jubair, W.K., Zanche, M., Meyers, J.R.*, et al.* (2019). Pro-inflammatory cytokine blockade attenuates myeloid expansion in a murine model of rheumatoid arthritis. Haematologica.

Isringhausen, S., Mun, Y., Kovtonyuk, L., Krautler, N.J., Suessbier, U., Gomariz, A., Spaltro, G., Helbling, P.M., Wong, H.C., Nagasawa, T.*, et al.* (2021). Chronic viral infections persistently alter marrow stroma and impair hematopoietic stem cell fitness. J Exp Med *218*.

Khosravi, A., Yanez, A., Price, J.G., Chow, A., Merad, M., Goodridge, H.S., and Mazmanian, S.K. (2014). Gut microbiota promote hematopoiesis to control bacterial infection. Cell Host Microbe *15*, 374-381.

Le Tortorec, A., Willey, S., and Neil, S.J. (2011). Antiviral inhibition of enveloped virus release by tetherin/BST-2: action and counteraction. Viruses *3*, 520-540.

Massberg, S., Schaerli, P., Knezevic-Maramica, I., Kollnberger, M., Tubo, N., Moseman, E.A., Huff, I.V., Junt, T., Wagers, A.J., Mazo, I.B.*, et al.* (2007). Immunosurveillance by Hematopoietic Progenitor Cells Trafficking through Blood, Lymph, and Peripheral Tissues. Cell *131*, 994-1008.

Matatall, K.A., Jeong, M., Chen, S., Sun, D., Chen, F., Mo, Q., Kimmel, M., and King, K.Y. (2016). Chronic Infection Depletes Hematopoietic Stem Cells through Stress-Induced Terminal Differentiation. Cell reports *17*, 2584-2595.

Mitroulis, I., Ruppova, K., Wang, B., Chen, L.S., Grzybek, M., Grinenko, T., Eugster, A., Troullinaki, M., Palladini, A., Kourtzelis, I.*, et al.* (2018). Modulation of Myelopoiesis Progenitors Is an Integral Component of Trained Immunity. Cell *172*, 147-161 e112.

Notario, L., Alari-Pahissa, E., Albentosa, A., Leiva, M., Sabio, G., and Lauzurica, P. (2018). Anti-CD69 therapy induces rapid mobilization and high proliferation of HSPCs through S1P and mTOR. Leukemia.

Pietras, E.M., Lakshminarasimhan, R., Techner, J.M., Fong, S., Flach, J., Binnewies, M., and Passegue, E. (2014). Re-entry into quiescence protects hematopoietic stem cells from the killing effect of chronic exposure to type I interferons. J Exp Med *211*, 245-262.

Pietras, E.M., Mirantes-Barbeito, C., Fong, S., Loeffler, D., Kovtonyuk, L.V., Zhang, S., Lakshminarasimhan, R., Chin, C.P., Techner, J.M., Will, B.*, et al.* (2016). Chronic interleukin-1 exposure drives haematopoietic stem cells towards precocious myeloid differentiation at the expense of self-renewal. Nat Cell Biol *18*, 607-618.

Poast, J., Seidel, H.M., Hendricks, M.D., Haslam, J.A., Levy, H.B., and Baron, S. (2002). Poly I:CLC induction of the interferon system in mice: an initial study of four detection methods. J Interferon Cytokine Res *22*, 1035-1040.

Rabe, J.L., Hernandez, G., Chavez, J.S., Mills, T.S., Nerlov, C., and Pietras, E.M. (2020). CD34 and EPCR coordinately enrich functional murine hematopoietic stem cells under normal and inflammatory conditions. Exp Hematol *81*, 1-15 e16.

Raveche, E.S., and Steinberg, A.D. (1982). Flow cytometric analysis of in vivo activation of murine spleen cells. J Immunopharmacol *4*, 163-181.

Rossi, D.J., Bryder, D., Zahn, J.M., Ahlenius, H., Sonu, R., Wagers, A.J., and Weissman, I.L. (2005). Cell intrinsic alterations underlie hematopoietic stem cell aging. Proceedings of the National Academy of Sciences of the United States of America *102*, 9194-9199.

Sato, T., Onai, N., Yoshihara, H., Arai, F., Suda, T., and Ohteki, T. (2009). Interferon regulatory factor-2 protects quiescent hematopoietic stem cells from type I interferon-dependent exhaustion. Nature medicine *15*, 696-700.

Sawai, C.M., Babovic, S., Upadhaya, S., Knapp, D.J., Lavin, Y., Lau, C.M., Goloborodko, A., Feng, J., Fujisaki, J., Ding, L.*, et al.* (2016). Hematopoietic Stem Cells Are the Major Source of Multilineage Hematopoiesis in Adult Animals. Immunity *45*, 597-609.

Takizawa, H., Fritsch, K., Kovtonyuk, L.V., Saito, Y., Yakkala, C., Jacobs, K., Ahuja, A.K., Lopes, M., Hausmann, A., Hardt, W.D.*, et al.* (2017). Pathogen-Induced TLR4-TRIF Innate Immune Signaling in Hematopoietic Stem Cells Promotes Proliferation but Reduces Competitive Fitness. Cell Stem Cell *21*, 225-240 e225.

Takizawa, H., Regoes, R.R., Boddupalli, C.S., Bonhoeffer, S., and Manz, M.G. (2011). Dynamic variation in cycling of hematopoietic stem cells in steady state and inflammation. J Exp Med *208*, 273-284.

Tough, D.F., Sun, S., and Sprent, J. (1997). T cell stimulation in vivo by lipopolysaccharide (LPS). J Exp Med *185*, 2089-2094.

van der Wath, R.C., Wilson, A., Laurenti, E., Trumpp, A., and Lio, P. (2009). Estimating dormant and active hematopoietic stem cell kinetics through extensive modeling of bromodeoxyuridine label-retaining cell dynamics. PloS one *4*, e6972.

Walter, D., Lier, A., Geiselhart, A., Thalheimer, F.B., Huntscha, S., Sobotta, M.C., Moehrle, B., Brocks, D., Bayindir, I., Kaschutnig, P.*, et al.* (2015). Exit from dormancy provokes DNA-damage-induced attrition in haematopoietic stem cells. Nature *520*, 549-552.

Yamamoto, R., Wilkinson, A.C., and Nakauchi, H. (2018). Changing concepts in hematopoietic stem cells. Science *362*, 895-896.

Yamashita, M., and Passegue, E. (2019). TNF-alpha Coordinates Hematopoietic Stem Cell Survival and Myeloid Regeneration. Cell Stem Cell *25*, 357-372 e357.

Yamazaki, S., Iwama, A., Morita, Y., Eto, K., Ema, H., and Nakauchi, H. (2007). Cytokine signaling, lipid raft clustering, and HSC hibernation. Ann N Y Acad Sci *1106*, 54-63.

Yanez, A., Murciano, C., O'Connor, J.E., Gozalbo, D., and Gil, M.L. (2009). Candida albicans triggers proliferation and differentiation of hematopoietic stem and progenitor cells by a MyD88-dependent signaling. Microbes and infection / Institut Pasteur *11*, 531-535.

Figures Caption

Figure 1. Immune activation of hematopoietic stem and progenitor cells is rapid

(A) Experimental plan with indicated pIpC stimulations and the different time points (0, 2, 4, and 24 h) in mice before analysis of BM.

(B) Representative FACS plots showing the percentage of CD69 and CD317 in the LSK (left panels) and HSC LSKCD48$^-$150$^+$ (right panels) populations from control and pIpC stimulated mice at different time points.

(C) Quantification of CD69 and CD317 expression in the LSK and HSC LSKCD48$^-$150$^+$ populations in the BM of control and pIpC stimulated mice.

(D) Experimental plan with indicated LPS stimulations in the different time points (0, 2, 4, and 24 h) in mice before analysis of BM.

(E) Representative FACS plots showing the percentage of CD69 and CD317 in the LSK (left panels), and HSC LSKCD48$^-$150$^+$ (right panels) populations from control and LPS stimulated mice at different time points.

(F) Quantification of CD69 and CD317 in the LSK and HSC LSKCD48$^-$150$^+$ populations in the BM of control and LPS stimulated mice.

Data are presented as average ± SD. Three independent experiments, n≥3 mice per group; significant p-values indicated *<0.05, **p<0.01and ***p<0.001.

Figure 2. CD317 reveals a dose-response to pIpC above a minimal threshold

(A) Representative FACS plots showing the percentage of CD317 in the LSK (upper panels) and HSC LSKCD48$^-$150$^+$ (lower panels) populations from the BM of PBS-control and pIpC stimulated mice under various pIpC doses (0.01 µg -100 µg as positive control) at 24 h.

(B and C) Quantification of the LSKCD317$^+$ and HSC LSKCD48$^-$150$^+$CD317$^+$ from the BM of PBS-control and different doses of pIpC stimulated mice.

(D and E) Linear regression model fitting the dose-response with the expression of CD317 in LSK and HSC LSKCD48$^-$150$^+$ populations. Solid lines represent the linear fit of data. Dotted lines represent Confidence intervals at 95%.

Data are presented as average ± SD. Three independent experiments, n≥3 mice per each group significant p-values indicated *<0.05, **p<0.01and ***p<0.001.

Figure 3. CD69 elevation is dose-dependent at higher concentrations of LPS stimulation

(A) Representative FACS plots showing the percentage of CD69 in the LSK (upper panels) and HSC LSKCD48$^-$150$^+$ (lower panels) populations from the BM of PBS-control and LPS stimulated mice, using various LPS doses (0.0001-20 µg as positive control) at 2 h.

(B and C) Quantification of $CD69^+$ expression in the LSK and HSC $LSKCD48^-150^+$ populations from PBS-control and LPS stimulated mice.

(D and E) Linear regression model fitting the dose-response with the expression of CD317 in LSK and HSC $LSKCD48^-150^+$ populations. Solid lines represent the linear fit of data. Dotted lines represent Confidence intervals at 95%.

Data are presented as average ± SD. Three independent experiments, n≥3 mice per each group significant p-values indicated *<0.05, **p<0.01and ***p<0.001.

Figure 4. CD69 and CD317 expression in activated stem and progenitor populations positively correlate with proliferation

(A) Representative FACS plot showing Ki67 cell cycle analysis of $LSKCD317^-$ and $LSKCD317^+$ from pIpC stimulated mice at 4 and 24 h time points.

(B and C) Quantification of cell cycle G0, G1, S, or M phases from $CD317^-/CD317^+$ fractions of the LSK and of HSC $LSKCD48^-150^+$ populations.

(D) Representative FACS plot showing the cell cycle analysis of $LSKCD69^-$ and $LSKCD69^+$ from LPS stimulated mice at 2 and 24 h time points.

(E-F) Quantification of cell cycle G0, G1, S, or M phases from $CD69^-/CD69^+$ fractions of the LSK and of HSC $LSKCD48^-150^+$ populations.

Data are presented as average ± SD. Three independent experiments, n≥3 mice per each group significant p-values indicated *<0.05, **p<0.01and ***p<0.001.

Figure 1

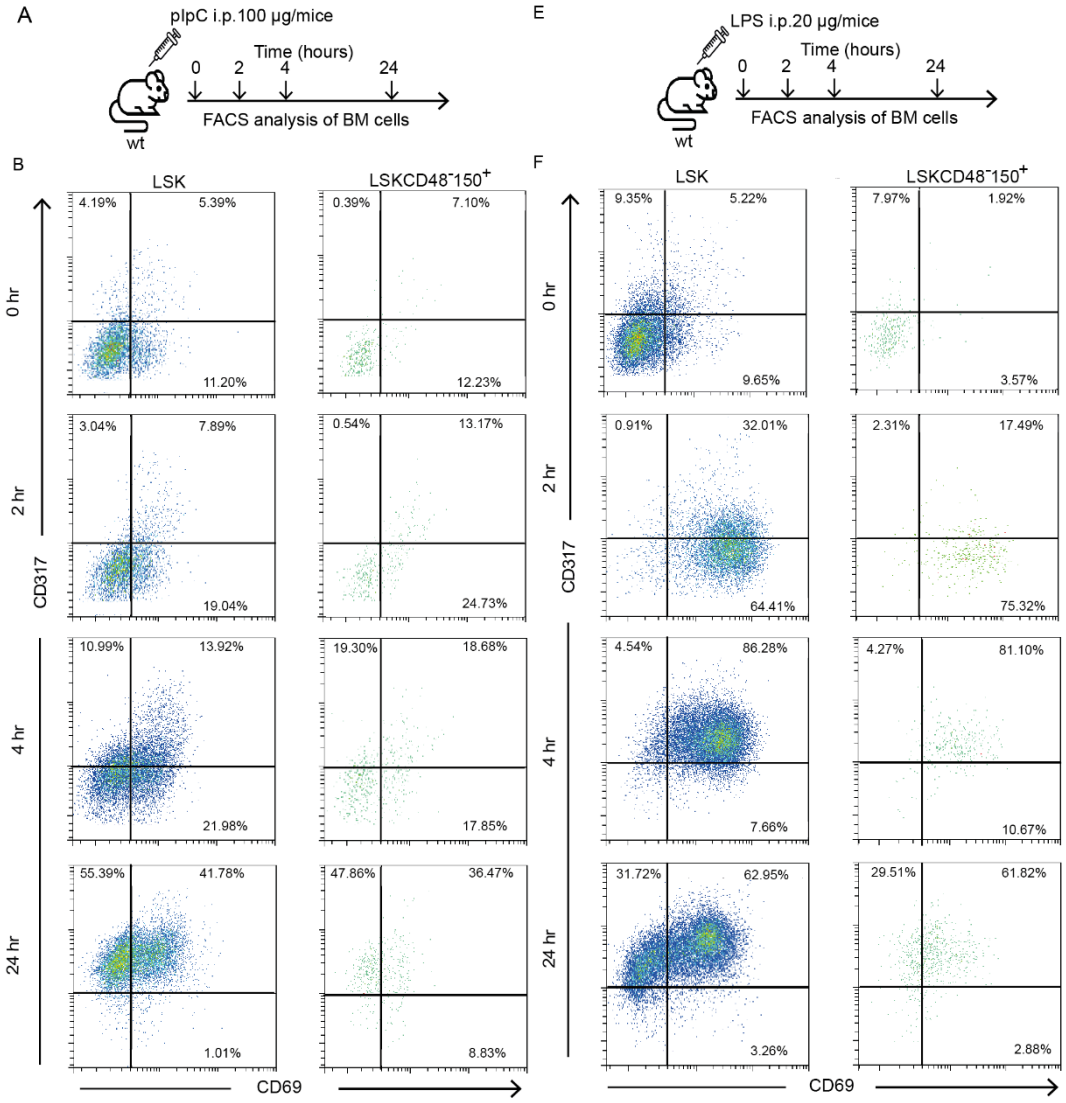
A
pIpC i.p.100 μg/mice
Time (hours)
0 2 4 24
FACS analysis of BM cells
wt
B
LSK
LSKCD48⁻150⁺
0 hr
2 hr
4 hr
24 hr
CD317
CD69
4.19% 5.39% 11.20%
0.39% 7.10% 12.23%
3.04% 7.89% 19.04%
0.54% 13.17% 24.73%
10.99% 13.92% 21.98%
19.30% 18.68% 17.85%
55.39% 41.78% 1.01%
47.86% 36.47% 8.83%
E
LPS i.p.20 μg/mice
Time (hours)
0 2 4 24
FACS analysis of BM cells
wt
F
LSK
LSKCD48⁻150⁺
0 hr
2 hr
4 hr
24 hr
CD317
CD69
9.35% 5.22% 9.65%
7.97% 1.92% 3.57%
0.91% 32.01% 64.41%
2.31% 17.49% 75.32%
4.54% 86.28% 7.66%
4.27% 81.10% 10.67%
31.72% 62.95% 3.26%
29.51% 61.82% 2.88%

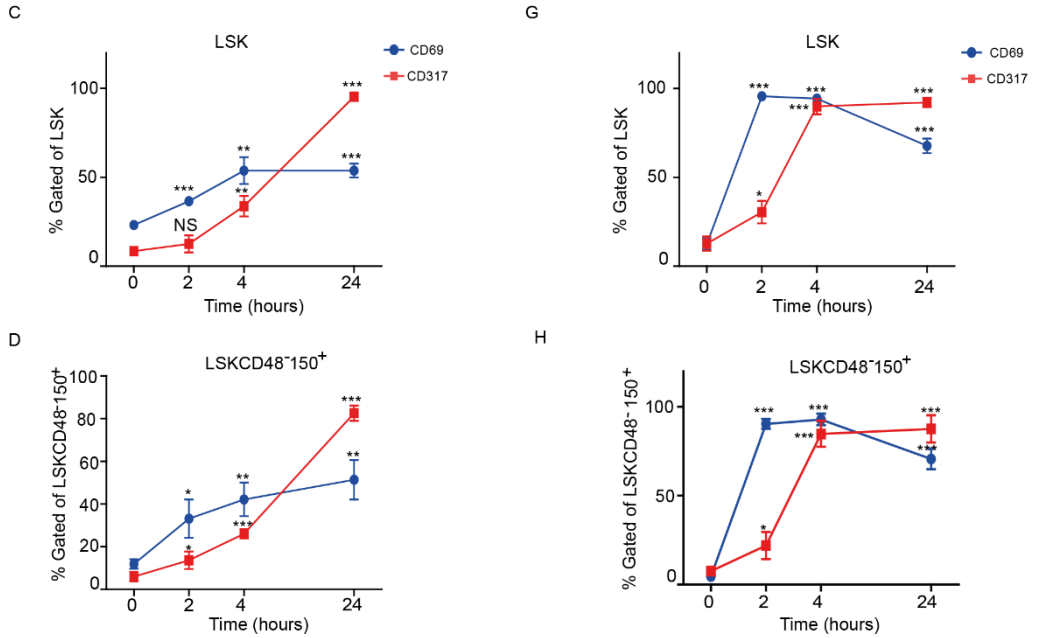
C
LSK
CD69
CD317
% Gated of LSK
Time (hours)
NS
D
LSKCD48⁻150⁺
% Gated of LSKCD48⁻150⁺
Time (hours)
G
LSK
CD69
CD317
% Gated of LSK
Time (hours)
H
LSKCD48⁻150⁺
% Gated of LSKCD48⁻150⁺
Time (hours)

Figure 2

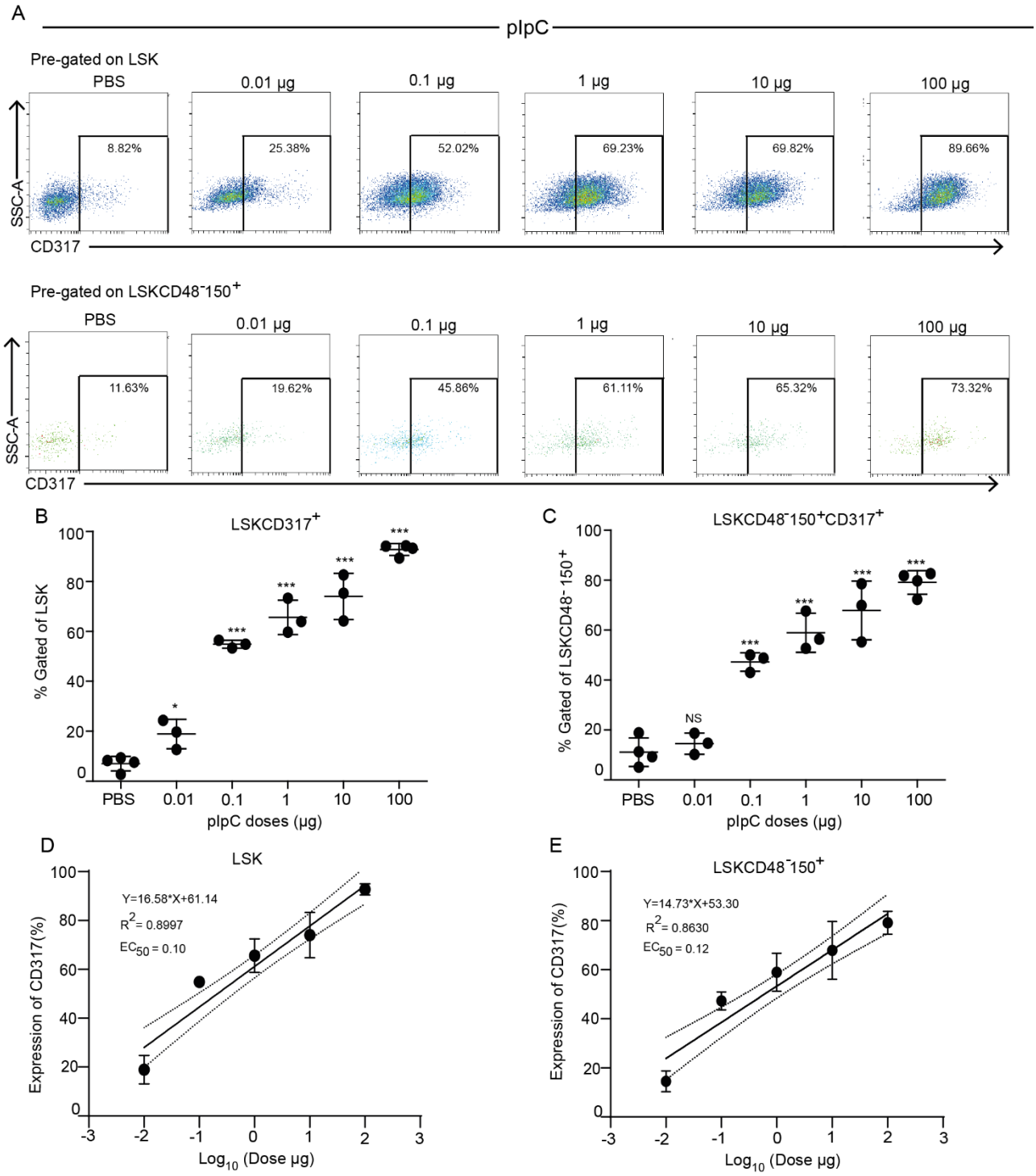
A
pIpC
Pre-gated on LSK
PBS
0.01 µg
0.1 µg
1 µg
10 µg
100 µg
8.82%
25.38%
52.02%
69.23%
69.82%
89.66%
SSC-A
CD317
Pre-gated on LSKCD48⁻150⁺
11.63%
19.62%
45.86%
61.11%
65.32%
73.32%
B
LSKCD317⁺
% Gated of LSK
pIpC doses (µg)
C
LSKCD48⁻150⁺CD317⁺
% Gated of LSKCD48⁻150⁺
NS
D
LSK
Y=16.58*X+61.14
R²= 0.8997
EC50 = 0.10
Expression of CD317(%)
Log10 (Dose µg)
E
LSKCD48⁻150⁺
Y=14.73*X+53.30
R²= 0.8630
EC50 = 0.12

Figure 3

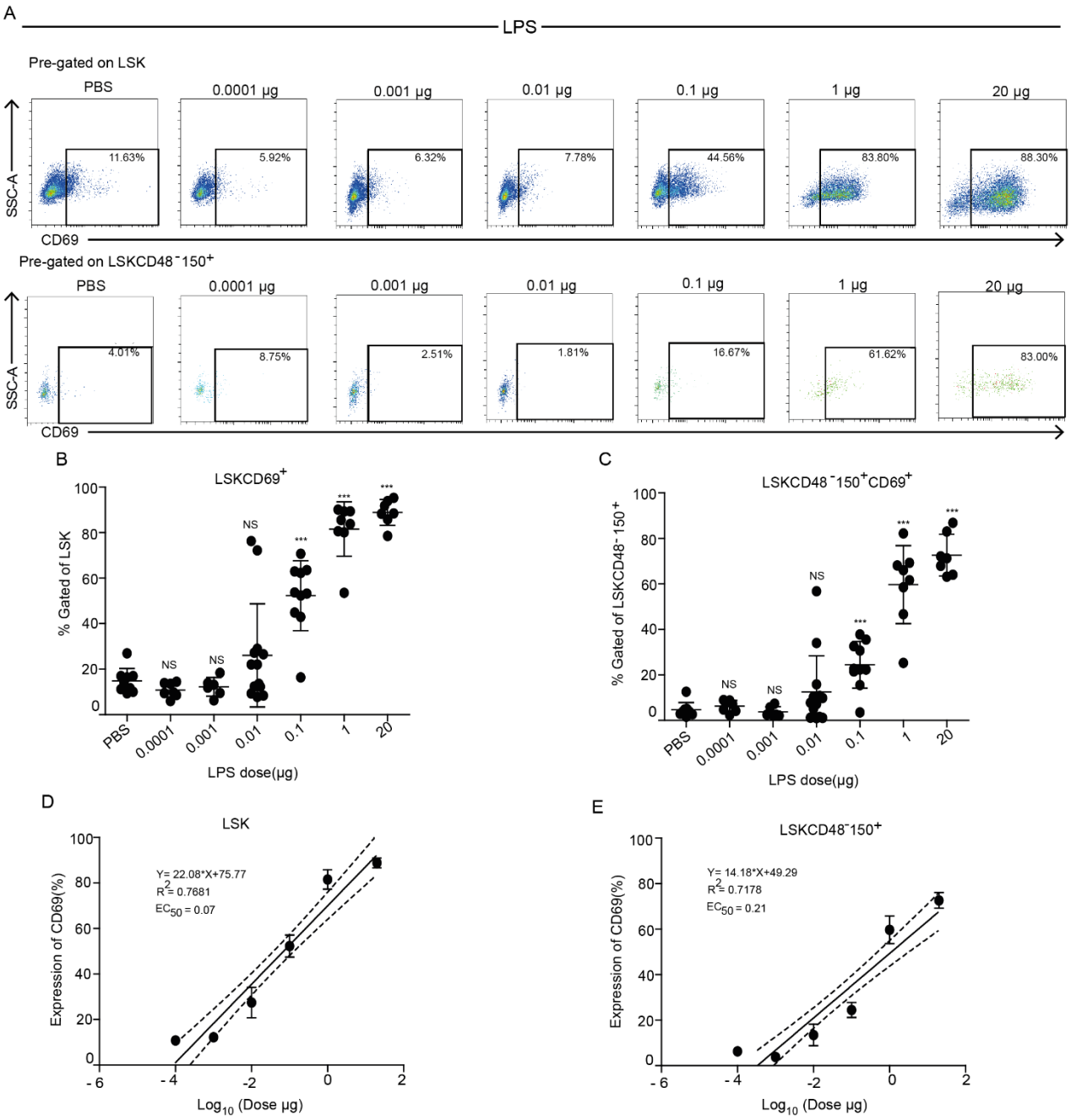
A
LPS
Pre-gated on LSK
PBS
0.0001 μg
0.001 μg
0.01 μg
0.1 μg
1 μg
20 μg
11.63%
5.92%
6.32%
7.78%
44.56%
83.80%
88.30%
SSC-A
CD69
Pre-gated on LSKCD48⁻150⁺
4.01%
8.75%
2.51%
1.81%
16.67%
61.62%
83.00%
B
LSKCD69⁺
% Gated of LSK
NS
***
PBS
0.0001
0.001
0.01
0.1
1
20
LPS dose(μg)
C
LSKCD48⁻150⁺CD69⁺
% Gated of LSKCD48⁻150⁺
D
LSK
Y= 22.08*X+75.77
R² = 0.7681
EC50 = 0.07
Expression of CD69(%)
Log10 (Dose μg)
E
LSKCD48⁻150⁺
Y= 14.18*X+49.29
R² = 0.7178
EC50 = 0.21

Figure 4

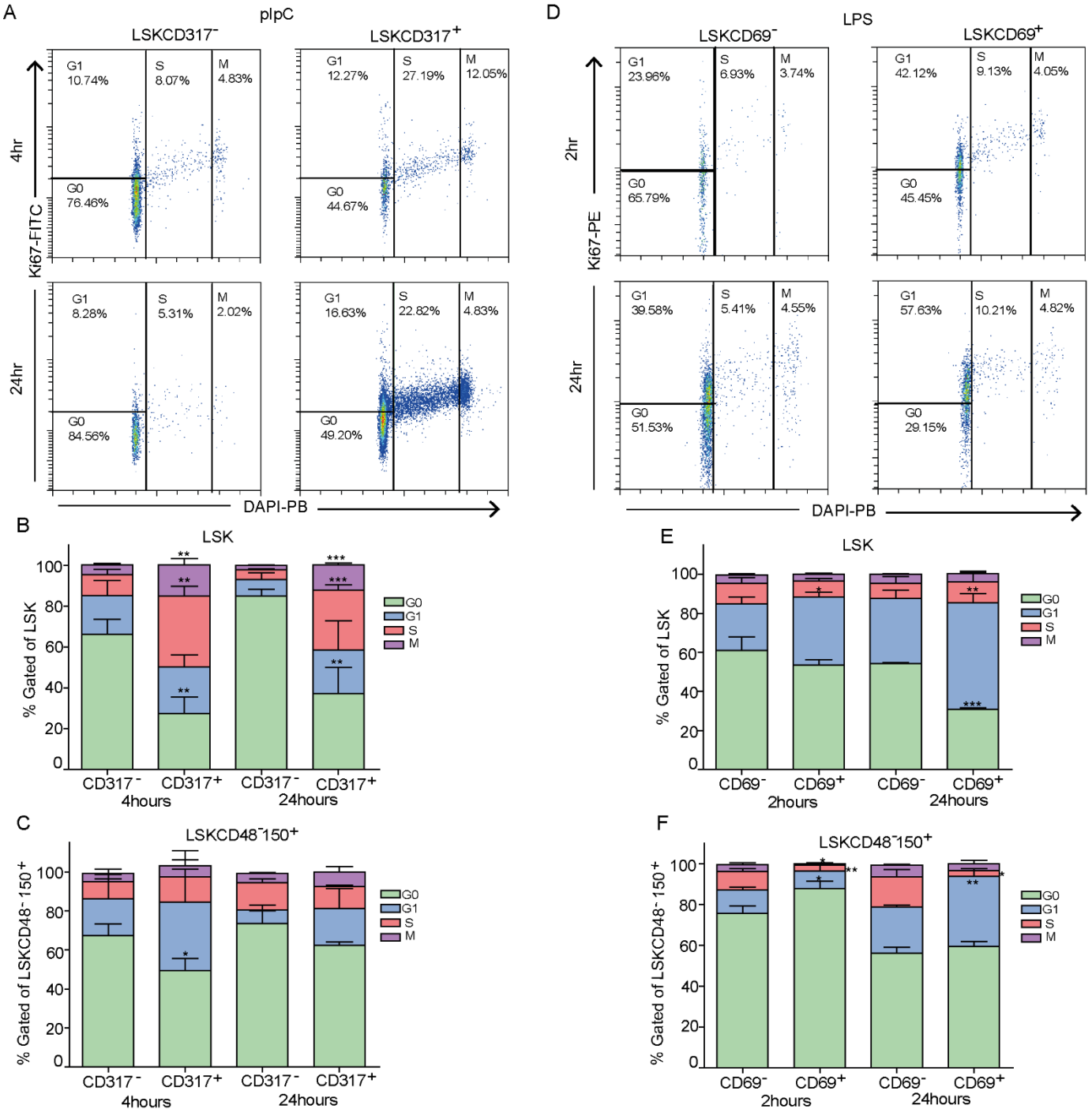
A
pIpC
LSKCD317⁻
LSKCD317⁺
4hr
24hr
Ki67-FITC
G1 10.74%
S 8.07%
M 4.83%
G0 76.46%
G1 12.27%
S 27.19%
M 12.05%
G0 44.67%
G1 8.28%
S 5.31%
M 2.02%
G0 84.56%
G1 16.63%
S 22.82%
M 4.83%
G0 49.20%
DAPI-PB
D
LPS
LSKCD69⁻
LSKCD69⁺
2hr
24hr
Ki67-PE
G1 23.96%
S 6.93%
M 3.74%
G0 65.79%
G1 42.12%
S 9.13%
M 4.05%
G0 45.45%
G1 39.58%
S 5.41%
M 4.55%
G0 51.53%
G1 57.63%
S 10.21%
M 4.82%
G0 29.15%
DAPI-PB
B
LSK
% Gated of LSK
G0
G1
S
M
CD317⁻ 4hours
CD317⁺
CD317⁻ 24hours
CD317⁺
E
LSK
% Gated of LSK
CD69⁻ 2hours
CD69⁺
CD69⁻ 24hours
CD69⁺
C
LSKCD48⁻150⁺
% Gated of LSKCD48⁻150⁺
CD317⁻ 4hours
CD317⁺
CD317⁻ 24hours
CD317⁺
F
LSKCD48⁻150⁺
% Gated of LSKCD48⁻150⁺
CD69⁻ 2hours
CD69⁺
CD69⁻ 24hours
CD69⁺

Supplemental Information

Supplemental Information Figures S1-S4

Figure S1, Related to Figure 1. Early activation of hematopoietic progenitors' cells,

(A) Experimental plan with indicated pIpC stimulations in the different time frames (0 h: PBS-control, 2 h 4 hours, and 24 h) in mice, and analysis of BM.

(B) Representative FACS plots showing the percentage of CD69 and CD317 in the Lineage$^-$ (Lin$^-$, left panels), and Lineage$^-$ cKit$^+$ (LK, right panels) populations from control and pIpC stimulated mice under different time points.

(C) Quantification of CD69 and CD317 Lin$^-$, left panels, and LK (right panels) populations from control and pIpC stimulated mice under different time points.

(D) Experimental plan with indicated LPS stimulations in the different time frames (control, 2, 4, and 24 hours) in mice and analysis of BM.

(E) Representative FACS plots showing the percentage of CD69 and CD317in the Lin$^-$ and LK populations from control and LPS stimulated mice at different time points.

(F) Quantification of CD69 and CD317 Lin$^-$ and LK populations from control and LPS stimulated mice at different time points.

Data are presented as average ± SD. Three independent experiments n≥3 mice per each group significant; p-values indicated *<0.05, **p<0.01and ***p<0.001.

Figure S2, Related to Figure 2. Dose-dependent effect of pIpC on hematopoietic progenitors' cells activation.

(A) Representative FACS plots showing the percentage of CD317 in the Lin populations (upper panels) and LK (lower panels) populations from the BM of PBS-control and pIpC treated mice under various pIpC doses (0.01 µg -100 µg as positive control) at 24h. (B and C) Quantification of the Lin$^-$CD317$^-$ (B) and LK CD317$^+$ of PBS-control and different doses of pIpC stimulated mice (C).

(D and E) The linear regression model fits the dose-response with the expression of CD317 in Lin$^-$ (D), and LK populations (E). Solid lines represent the linear fit of data. Dotted lines represent Confidence intervals at 95%.

Data are presented as average ± SD. Three independent experiments, n≥3 mice per each group; significant p-values indicated *<0.05, **p<0.01and ***p<0.001.

Figure S3, Related to Figure 3. Hematopoietic progenitor cells activation is not dose-dependent.

(A) Representative FACS plots showing the percentage of CD69 in the Lineage$^-$ (Lin$^-$) populations (upper panels) and LK populations (lower panels) populations from the BM of PBS-control and LPS stimulated mice under various LPS doses (0.01 µg -100 µg as positive control) at 2h.

(B and C) Quantification of the Lin$^-$CD69$^-$ (B) and LK CD69$^+$ of PBS-control and different doses of pIpC stimulated mice (C).

(D and E) The linear regression model of the dose-response with the expression of CD69 in Lin$^-$ (D), and LK populations (E). Solid lines represent the linear fit of data. Dotted lines represent Confidence intervals at 95%.

Data are presented as average ± SD. Three independent experiments, n≥3 mice per each group; significant p-values indicated *<0.05, **p<0.01and ***p<0.001.

Figure S4, Related to Figure 4. Hematopoietic stem cell and progenitor activation is linked with proliferation.

(A) Representative FACS plot showing the cell cycle analysis of Lin$^-$CD317$^-$ / Lin$^-$CD317$^+$ (upper panels) and LKCD317$^-$ / LKCD317$^+$ (lower panels) from pIpC stimulated mice at 4 and 24htime points.

(B and C) Quantification of cell cycle G0, G1, S, or M phases from Lin$^-$CD317$^-$ and Lin$^-$CD317$^+$ (B) and LKCD317$^-$ and LKCD317$^+$ populations (C).

(D) Representative FACS plot showing the cell cycle analysis of Lin$^-$CD69$^-$ / Lin$^-$CD69$^+$ (upper panels) and LKCD69$^-$ / LKCD69$^+$ (lower panels) from LPS stimulated mice at 2 and 24 h.

(E-F) Quantification of cell cycle G0, G1, S, or M phases from Lin$^-$CD69$^-$ and Lin$^-$CD69$^+$ (E). LKCD69$^-$ and LKCD69$^+$ populations (F).

Data are presented as average ± SD. Three independent experiments, n≥3 mice per each group; significant p-values indicated *<0.05, **p<0.01and ***p<0.001.

Figure S1

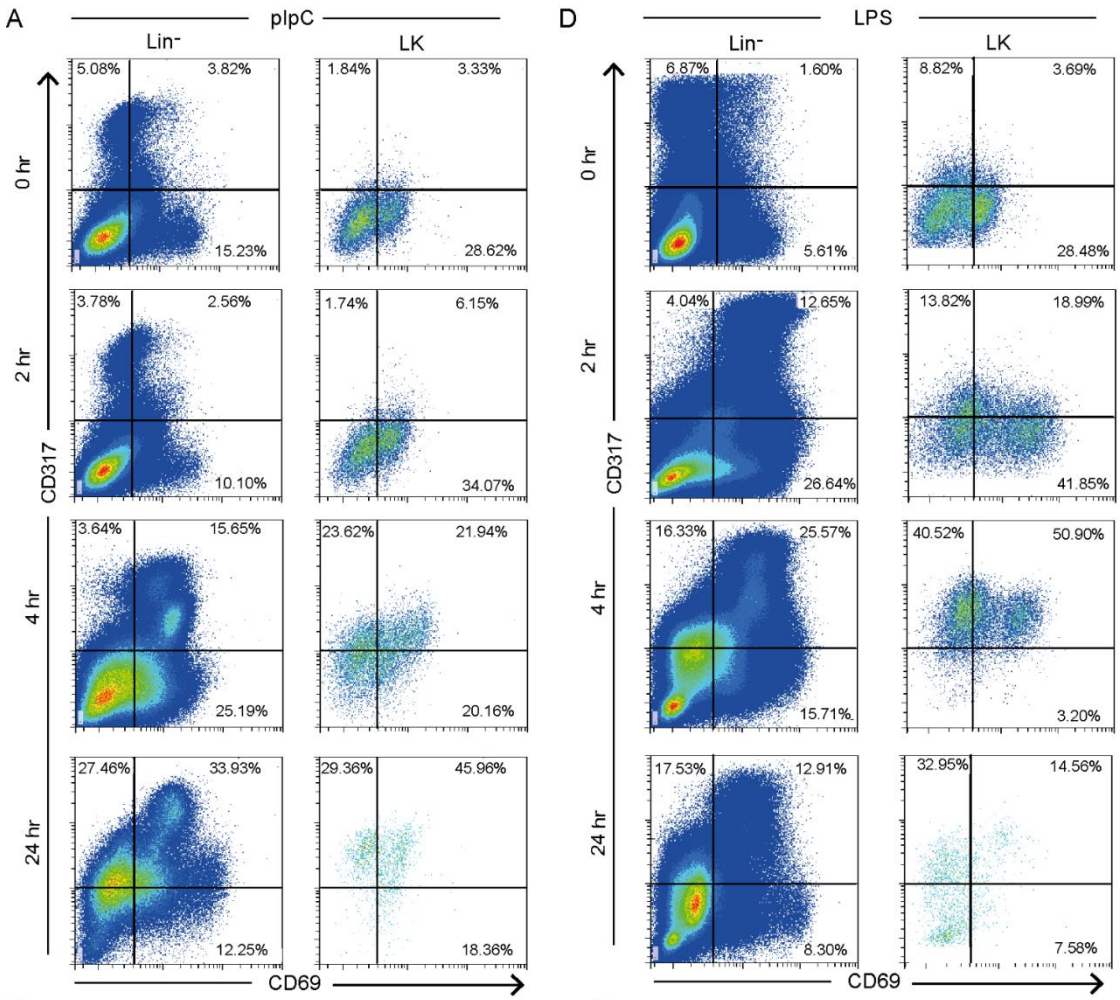
A
pIpC
Lin-
LK
0 hr
2 hr
4 hr
24 hr
CD317
CD69
5.08%
3.82%
15.23%
1.84%
3.33%
28.62%
3.78%
2.56%
10.10%
1.74%
6.15%
34.07%
3.64%
15.65%
25.19%
23.62%
21.94%
20.16%
27.46%
33.93%
12.25%
29.36%
45.96%
18.36%
D
LPS
6.87%
1.60%
5.61%
8.82%
3.69%
28.48%
4.04%
12.65%
26.64%
13.82%
18.99%
41.85%
16.33%
25.57%
15.71%
40.52%
50.90%
3.20%
17.53%
12.91%
8.30%
32.95%
14.56%
7.58%

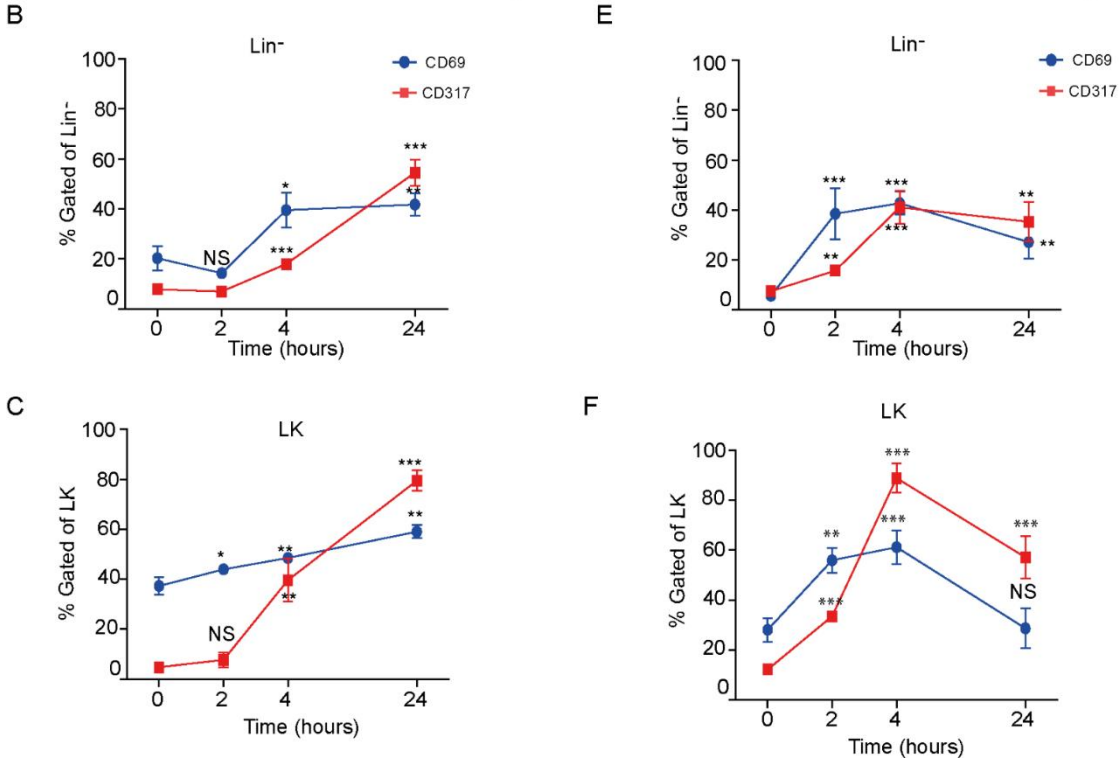
B
Lin-
CD69
CD317
% Gated of Lin-
Time (hours)
NS
C
LK
% Gated of LK
E
F
NS

Figure S2

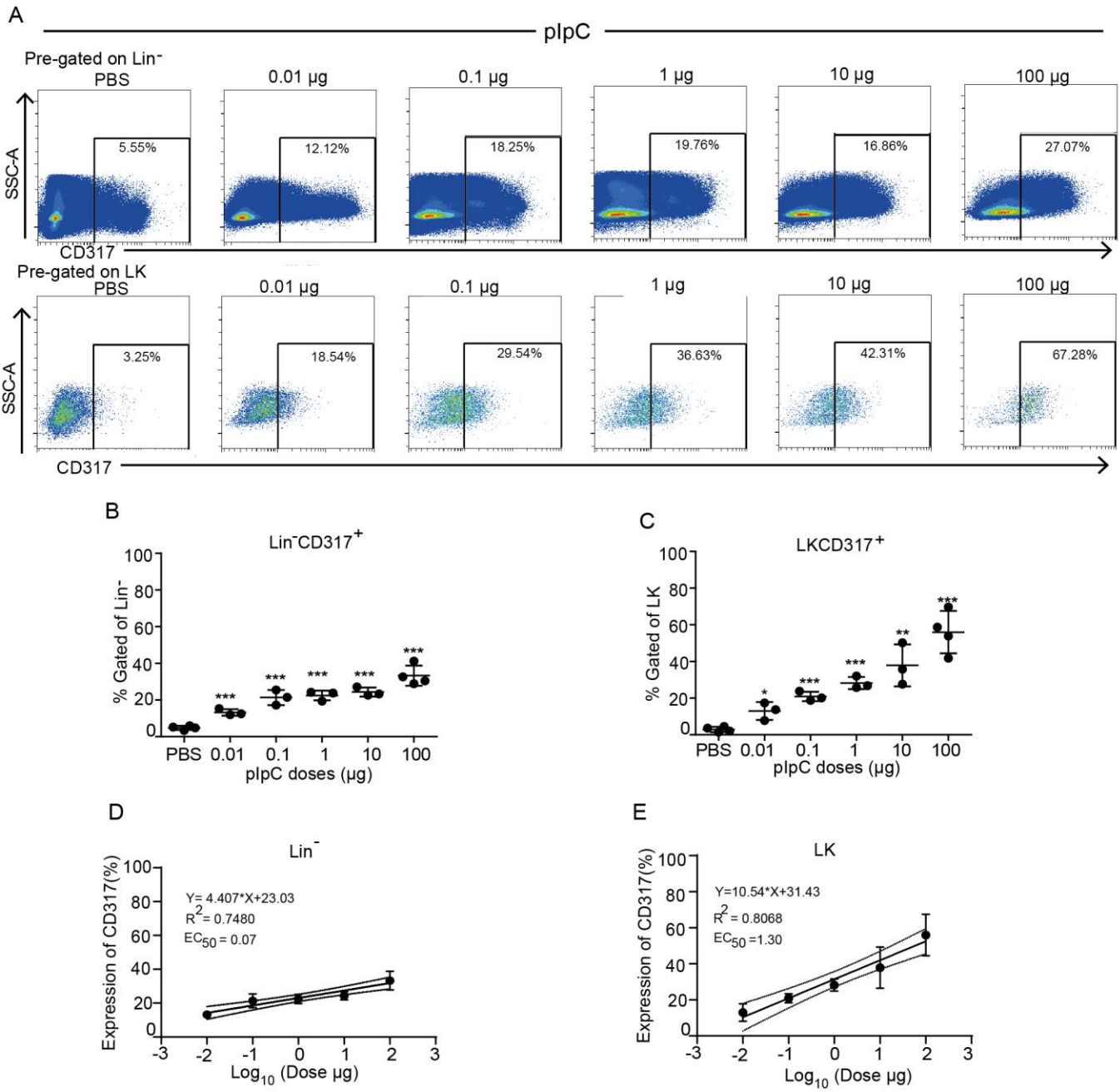
A
pIpC
Pre-gated on Lin⁻
PBS
0.01 µg
0.1 µg
1 µg
10 µg
100 µg
5.55%
12.12%
18.25%
19.76%
16.86%
27.07%
SSC-A
CD317
Pre-gated on LK
3.25%
18.54%
29.54%
36.63%
42.31%
67.28%
B
Lin⁻CD317⁺
% Gated of Lin⁻
pIpC doses (µg)
C
LKCD317⁺
% Gated of LK
D
Lin⁻
Y= 4.407*X+23.03
R² = 0.7480
EC50 = 0.07
Expression of CD317(%)
Log10 (Dose µg)
E
LK
Y=10.54*X+31.43
R² = 0.8068
EC50 =1.30

Figure S3

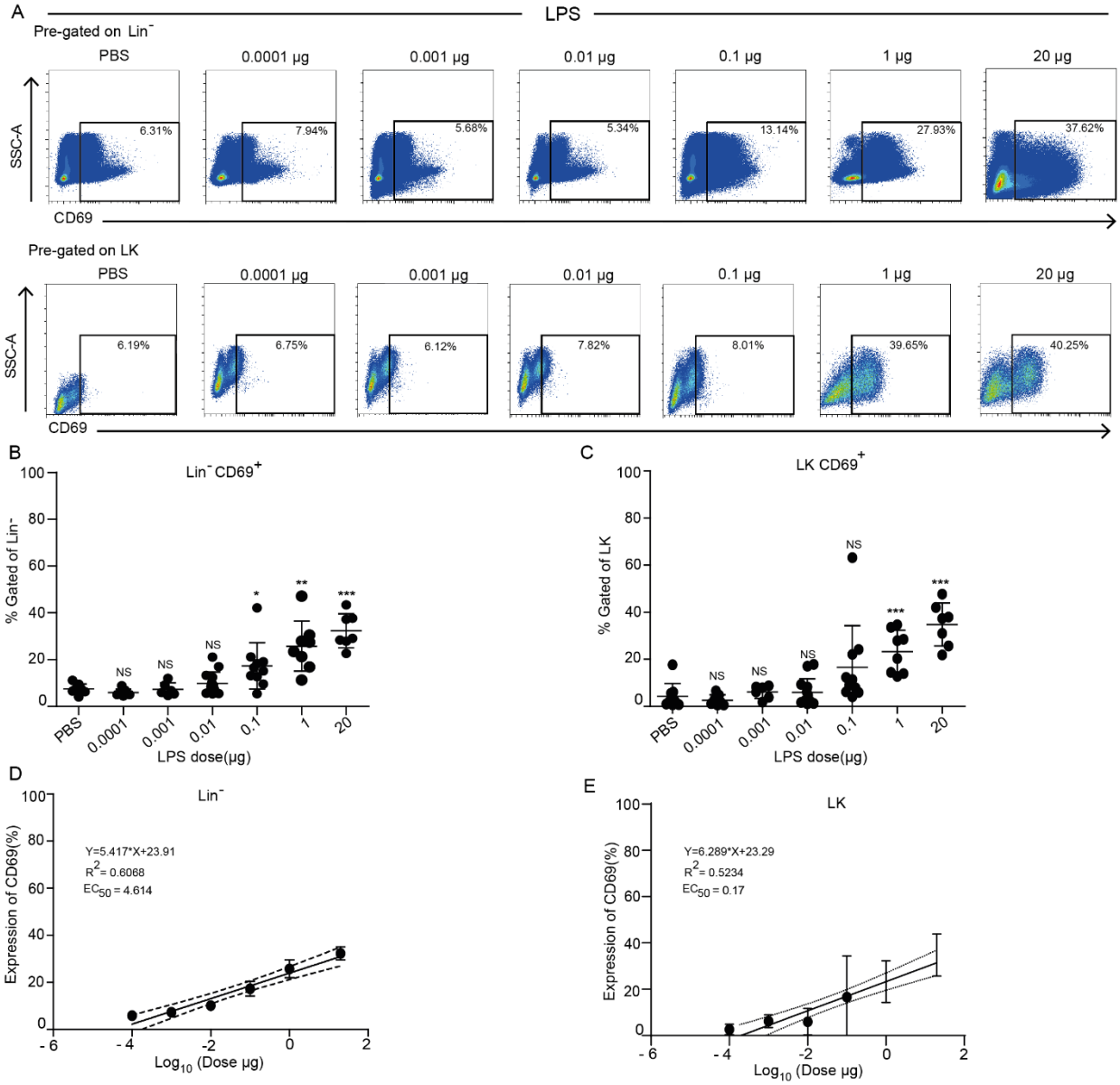
A
LPS
Pre-gated on Lin⁻
PBS
0.0001 μg
0.001 μg
0.01 μg
0.1 μg
1 μg
20 μg
SSC-A
CD69
6.31%
7.94%
5.68%
5.34%
13.14%
27.93%
37.62%
Pre-gated on LK
6.19%
6.75%
6.12%
7.82%
8.01%
39.65%
40.25%
B
Lin⁻CD69⁺
% Gated of Lin⁻
LPS dose(μg)
C
LK CD69⁺
% Gated of LK
D
Lin⁻
Y=5.417*X+23.91
R²= 0.6068
EC50 = 4.614
Expression of CD69(%)
Log10 (Dose μg)
E
LK
Y=6.289*X+23.29
R²= 0.5234
EC50 = 0.17

Figure S4

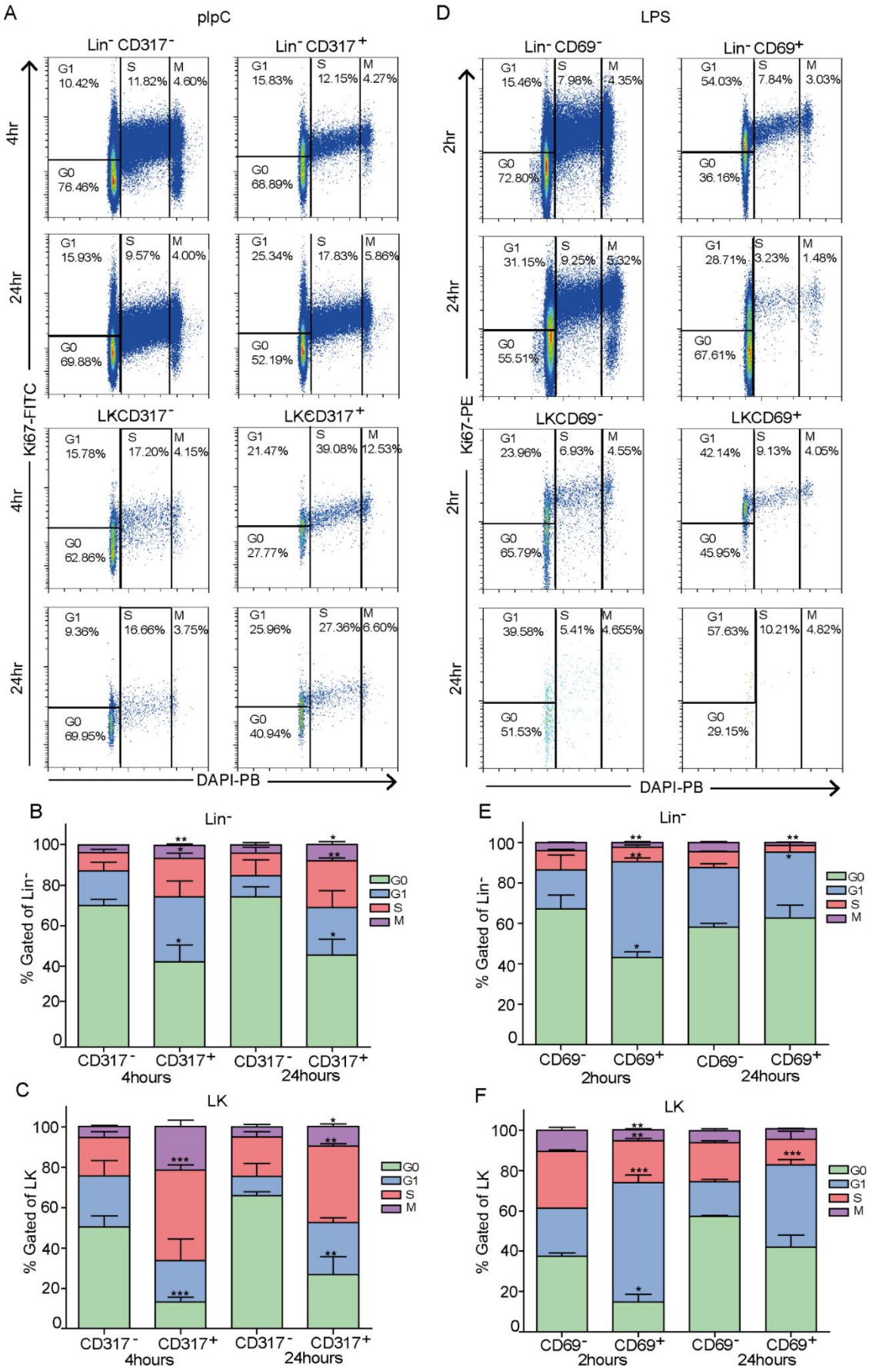
A
pIpC
Lin⁻ CD317⁻
Lin⁻ CD317⁺
4hr
24hr
G1 10.42%
S 11.82%
M 4.60%
G0 76.46%
G1 15.83%
S 12.15%
M 4.27%
G0 68.89%
G1 15.93%
S 9.57%
M 4.00%
G0 69.88%
G1 25.34%
S 17.83%
M 5.86%
G0 52.19%
LKCD317⁻
LKCD317⁺
G1 15.78%
S 17.20%
M 4.15%
G0 62.86%
G1 21.47%
S 39.08%
M 12.53%
G0 27.77%
G1 9.36%
S 16.66%
M 3.75%
G0 69.95%
G1 25.96%
S 27.36%
M 6.60%
G0 40.94%
Ki67-FITC
DAPI-PB
D
LPS
Lin⁻ CD69⁻
Lin⁻ CD69⁺
2hr
24hr
G1 15.46%
S 7.98%
M 4.35%
G0 72.80%
G1 54.03%
S 7.84%
M 3.03%
G0 36.16%
G1 31.15%
S 9.25%
M 5.32%
G0 55.51%
G1 28.71%
S 3.23%
M 1.48%
G0 67.61%
LKCD69⁻
LKCD69⁺
G1 23.96%
S 6.93%
M 4.55%
G0 65.79%
G1 42.14%
S 9.13%
M 4.05%
G0 45.95%
G1 39.58%
S 5.41%
M 4.655%
G0 51.53%
G1 57.63%
S 10.21%
M 4.82%
G0 29.15%
Ki67-PE
DAPI-PB
B
Lin⁻
% Gated of Lin⁻
CD317⁻
CD317⁺
4hours
24hours
G0
G1
S
M
C
LK
% Gated of LK
E
Lin⁻
CD69⁻
CD69⁺
2hours
24hours
F
LK